Formalism for multiphoton plasmon excitation in jellium clusters

Jean-Patrick Connerade*
The Blackett Laboratory, Imperial College, London SW7 2BW, United Kingdom

Andrey V. Solov'yov†
A.F. Ioffe Physical-Technical Institute of the Academy of Sciences of Russia, Polytechnicheskaya 26, St. Petersburg 194021, Russia
(Received 1 March 2002; published 29 July 2002)

We present a formalism for the description of multiphoton plasmon excitation processes in jellium clusters. By using our method, we demonstrate that, in addition to dipole plasmon excitations, the multipole plasmons (quadrupole, octupole, etc.) can be excited in a cluster by multiphoton absorption processes, which results in a significant difference between plasmon resonance profiles in the cross sections for multiphoton as compared to single-photon absorption. We calculate the cross sections for multiphoton absorption and analyze the balance between the surface and volume plasmon contributions to multipole plasmons.

DOI: 10.1103/PhysRevA.66.013207 PACS number(s): 36.40.Gk

I. INTRODUCTION

In the present paper we demonstrate that, in addition to dipole plasmon excitations, multipole plasmons (quadrupole, octupole, etc.) contribute to the multiphoton excitation process, which results in a significant difference of plasmon resonance profiles between the cross sections for multiphoton and single-photon absorption. We have developed a formalism from which the cross sections for multiphoton excitation can be worked out. The balance between multipole surface and volume-plasmon contributions is analyzed. Our results are obtained within a theoretical model for the multiphoton excitation of a jellium cluster. This model is applicable to metal clusters, to fullerenes, and to any type of cluster in which a strong delocalization of valence atomic orbitals occurs. The theoretical formalism we have developed is not confined in its application to photons. It can also be used to describe any kind of higher-order plasmon excitation processes, for example, those which arise by multiple scattering of electrons within the cluster.

It is important to note that we use the jellium framework for simplicity. In fact, all the conclusions regarding selection rules and the general behavior of single versus multiphoton cross section are model independent. So, the jellium calculations are used in our work merely as an illustration of what happens when the general formulas are applied. Although, there is no real physical system which follows the jellium calculations, just as there is no atom which really follows pure Hartree-Fock calculations. Nevertheless, the Hartree-Fock method is important (as is the jellium method) in providing an intellectual framework within which the fundamental physical interactions can be clearly distinguished, as well as a basis for more elaborate computations, for example, of correlations and exchange. Physics often appeals to models that are not strictly applicable to real situations, but are nevertheless fundamental. Actually, this is a prime feature of many-body systems. Very realistic models usually achieve their success at the expense of an increase in complexity which introduces uncertainties of interpretation.

Recently, a number of papers have discussed metallic clusters [1,2] and fullerenes [3] in strong laser fields. The theoretical approach usually followed is to solve a time-dependent local-density equation numerically (LDA or local-density approximation), and the regime most commonly studied involves intense, short laser pulses, for which the turn-on and turn-off properties significantly affect excitation.

We report here on a different problem: our initial interest lies in lower laser powers, for which multiphoton excitation just begins to intrude, and we are interested in developing a formalism to describe the interaction between collective modes and a laser field in the multiphoton regime. For this purpose, a semiclassical model, in which the collective flow of charge is driven by a periodic field, is established, and we relate it to the multiphoton absorption cross section of the cluster, which takes into account quantum mechanics. Of course, one can in principle extend this treatment to include the turn on and turn off of laser pulses, to treat the interaction numerically for various power levels and initial charge distributions. What we wish to point out, however, is an important feature, which arises even for an infinite wave train interacting with a cluster (the simplest and most fundamental problem): multiple plasmon excitations are driven by multiphoton excitations. In the present paper, we explain by what mechanism this arises.

Our approach is based on principles different from the LDA. Instead of using the Kohn-Sham formalism, we propose a hydrodynamic approach. In the LDA, all quantities are made to depend solely on charge density, and currents are subsequently made to appear by solving a time-dependent equation. In our approach, we start from the continuity equation and the Euler equation, from which both the current flow and the density are obtained in a completely consistent way. Our theory is local, and does not include exchange. In principle, it would be possible to extend it by building in exchange and correlations in a way similar to the LDA. One of the benefits of our approach is that all the momentum-transfer terms are included in the formulation, which leads to the presence of both volume and surface plasmon terms. If

*Email address: j.connerade@ic.ac.uk
†Email address: solovyov@rpro.ioffe.rssi.ru

one wishes to simplify the theory, it is possible towards the end of the calculation to assume zero momentum transfer, in which case the volume-plasmon terms disappear from the problem.

Surface-plasmon excitations are well known in atomic cluster physics. The dipole surface plasmons are responsible for the formation of giant resonances in photoabsorption spectra of metal clusters (see, e.g., Refs. [4–12]). They also play an important role in inelastic collisions of charged particles with metal clusters [13–19]. The role of surface plasmon excitations in inelastic electron-cluster scattering was thoroughly studied in [13,17–19], and it was demonstrated that collective excitations contribute significantly to the electron energy loss spectrum in the region of the surface-plasmon resonance. With increasing scattering angle, plasmon excitations of higher angular momenta become more and more prominent.

Plasmons are characteristic of delocalized electrons, and therefore the jellium model provides the most appropriate starting point for a discussion of plasmon excitation in the multiphoton regime. This regime is particularly appropriate for the study of atomic clusters, which are rather fragile objects, and readily explode under very strong irradiation [20].

The inelastic scattering of fast electrons on metal clusters in the range of transferred energies above the ionization threshold was considered in Ref. [21]. It was demonstrated that, in this energy range, volume plasmons dominate the contribution to the differential cross section, resulting in a resonance behavior. The volume-plasmon resonances excited in the cluster during a collision decay via the ionization process. The resonance frequency and the autoionization width of the volume-plasmon excitations have both been determined in Ref. [21]. In this work the results of the plasmon resonance approximation for fast electrons scattering on sodium clusters have been compared with those following from the *ab initio* quantum treatment performed within the random-phase approximation with exchange. This comparison demonstrated quite reasonable applicability of the plasmon resonance approximation, i.e., the jellium model, to this problem. This fact leads us to the conclusion that one can expect the same level of accuracy of the theory based on the jellium principles in other relevant physical situations, such as multiphoton absorption processes.

The role of the polarization interaction and plasmon excitations in the process of electron attachment to metal clusters has also been examined both theoretically [22,23] and experimentally [24]. It was demonstrated that plasmon excitations induce a resonance enhancement of the electron attachment cross section.

Our paper is organized as follows. In Sec. II, we derive quantum-mechanical expressions for the cross sections of multipole (quadrupole, octupole, etc.) plasmon excitations taking place in the multiphoton absorption regime and estimate the cross sections on the basis of the plasmon resonance approximation. We present and discuss the multiphoton absorption profiles and demonstrate a significant change of the profiles in the cross sections for multiphoton as compared to single-photon absorption. In Sec. III, we establish certain connections of the cross sections with the variation of electron density in the cluster due to the external field and present the formalism for the calculation of the electron-density variation in the cluster due to the external field, based on the the hydrodynamic Euler equation and on the equation of continuity. We apply the general formalism to the description of fast electron-cluster scattering and multiphoton absorption. In Sec. IV, we calculate the multipole moments of the system induced by the external field on the basis of the formalism outlined in Sec. III. We analyze the plasmon resonance structure of the induced multipole moments and conclude that it is analogous to the one arising in the multiphoton absorption cross sections calculated in Sec. II. In Sec. V, we draw conclusions from this work. In Appendix A, we show how matrix elements for collective transitions can be calculated on the basis of the sum rules. In Appendix B, we present details of calculations of the angular integrals arising in the formalism outlined here.

II. PLASMON RESONANCE APPROXIMATION FOR MULTIPHOTON ABSORPTION CROSS SECTIONS

First, we consider the cross section for multiphoton absorption in jellium clusters and demonstrate that multipole plasmon excitations are essential to this process. The discussion in this section is based on the plasmon resonance approximation, which is introduced below.

A. Single-photon absorption

Let us start by considering the simplest example and calculate the cross section for single-photon absorption in the plasmon resonance approximation.

The single-photon absorption cross section in the dipole approximation reads as

$$\sigma_1 = \frac{4\pi^2 e^2}{c}\omega \sum_n |z_{on}|^2 \delta(\omega_{no} - \hbar\omega). \tag{1}$$

Here, e is the charge of electron, c is the velocity of light, $\hbar$ is Planck's constant, $\omega_{no} = \varepsilon_n - \varepsilon_0$ is the electron excitation energy, ω is the photon frequency, and ez_{on} is the matrix element of the z component of the cluster dipole moment. The summation over n includes all final states of the excited electron, which belong to both the discrete and the continuous spectra.

In the jellium picture, which works reasonably well for metal clusters and to some extent for fullerenes, the main contribution to the cross section (1) arises from a small group of excited states or sometimes even from a single transition close in frequency to the classical Mie resonance—also known as the plasmon resonance. For a spherical metal cluster, this frequency is given by (see, e.g., Refs. [10,17] and Sec. IV of this paper)

$$\omega_l^2 = \frac{4\pi N e^2}{mV}\frac{l}{(2l+1)}. \tag{2}$$

Here $V = 4\pi R^3/3$ is the cluster volume, where $R = r_o N^{1/3}$ is the cluster radius, r_o is the Wigner-Seitz radius; N is the number of delocalized electrons in a cluster, l is the

angular momentum of the plasmon mode, m is the electron mass. Note that, by using a single photon of energy 1–4 eV, one can, in practice, excite only $l=1$ dipole plasmon oscillations in a metallic cluster.

For nearly spherical fullerenes C_{20} or C_{60}, the plasmon resonance frequency is (see Refs. [11,17])

$$\omega_l^2=\frac{l(l+1)N}{(2l+1)R^3}, \tag{3}$$

where N is the total number of delocalized electrons (four electrons per atom times the number of carbon atoms in the fullerene molecule) and R is the the radius of the fullerene.

The plasmon resonance approximation is based on the fact that excitations near a plasmon resonance exhaust the sum rule almost completely (see Refs. [4–7,10,11]), which means that the summation in the sum rule (see, e.g., Ref. [25])

$$\sum_n \omega_{no}|z_{on}|^2=\frac{N\hbar^2}{2m} \tag{4}$$

need only be performed over excited states near the Mie resonance.

Now, assuming a Lorentzian distribution of width Γ_1 for the plasmon resonance states and replacing the δ function, $\delta(\omega_{no}-\hbar\omega)$, in Eq. (1) by the profile (see, e.g., Ref. [25])

$$\delta(\omega_{no}-\hbar\omega)\to\frac{\Gamma_1}{2\pi\hbar\left((\omega_1-\omega)^2+\frac{\Gamma_1^2}{4}\right)}, \tag{5}$$

one recovers the well-known expression for the single-photon absorption cross section (see, e.g., Refs. [4,10])

$$\sigma_1=\frac{\pi Ne^2}{mc}\frac{\Gamma_1}{(\omega_1-\omega)^2+\frac{\Gamma_1^2}{4}}\approx\frac{4\pi Ne^2}{mc}\frac{\omega^2\Gamma_1}{(\omega_1^2-\omega^2)^2+\omega^2\Gamma_1^2}. \tag{6}$$

The width Γ_1 is due to Landau damping. Its calculation for metal clusters is performed, for example, in Ref. [21].

The cross section (6) reproduces correctly the appearance of plasmon resonances in single-photon absorption spectra of metal clusters and fullerenes, although some details of the experimentally observed profiles are naturally beyond the plasmon resonance approximation. The discussion of these details is also beyond the scope of the present paper. They can only be treated accurately enough on the basis of *ab initio* many-body theories. Instead, we analyze the multiphoton absorption cross section on the basis of the plasmon resonance approximation and elucidate the role of multipole plasmon excitations, because our interest lies in establishing the physical mechanisms of multiphoton excitation.

B. Two-photon absorption

In the dipole approximation, the two-photon absorption cross section is

$$\sigma_2=\frac{32\pi^3e^4\hbar}{c^2}\omega^2\sum_n\left|\sum_m\frac{z_{nm}z_{mo}}{\hbar\omega-\omega_{mo}+i\delta}\right|^2\delta(\omega_{no}-2\hbar\omega). \tag{7}$$

We evaluate the cross section (7) in the same way as for the single-photon case. The main contribution to the sum over the intermediate states m arises from the virtual dipole plasmon excitations. Therefore, one derives

$$\sum_n\left|\sum_m\frac{z_{nm}z_{mo}}{\hbar\omega-\omega_{mo}+i\delta}\right|^2\approx\frac{N}{2m\hbar\omega_1}\sum_n\frac{|z_{n1}|^2}{(\omega-\omega_1)^2+\Gamma_1^2/4}. \tag{8}$$

Here, we have also introduced a dipole plasmon resonance width Γ_1 and used the sum rule (4) for the evaluation of the matrix elements for dipole plasmon excitation $|r_{10}|^2\approx N\hbar/2m\omega_1$. The remaining matrix elements z_{n1} in Eq. (8) describe dipole transitions from the dipole plasmon resonance state to other excited states. Matrix elements for these transitions obey the dipole selection rule. This means that the angular momentum of the final state can be only $l=0$ or $l=2$. According to Eqs. (2) and (3), there is no surface-plasmon excitation with $l=0$ either in metal clusters or in fullerenes. Thus, only transitions to states with $l=2$ are of interest.

These arguments show that, by using two photons simultaneously, one can excite the quadrupole plasmon resonance in a metal cluster or in a fullerene with a frequency given in Eqs. (2) and (3), respectively. When calculating the cross section (7) near the quadrupole plasmon resonance excitation, i.e., at $2\omega\sim\omega_2$, it is sufficient to consider only transitions to the resonance final state, i.e., to put $\Sigma_n|z_{n1}|^2\approx|z_{21}|^2$ (here and below we use indices 1 and 2 to designate the dipole and quadrupole plasmon resonance states) and to replace the δ function, $\delta(\omega_{no}-2\hbar\omega)$, by a Lorentzian distribution of width Γ_2 (see, e.g., Ref. [25]),

$$\delta(\omega_{no}-2\hbar\omega)\to\frac{\Gamma_2}{2\pi\hbar\left((\omega_2-2\omega)^2+\frac{\Gamma_2^2}{4}\right)}. \tag{9}$$

By substituting Eqs. (8) and (9) in Eq. (7), one derives

$$\sigma_2=\left(\frac{4\pi Ne^2}{mc}\right)^2\frac{m|z_{21}|^2}{2N\hbar\omega_1}\frac{\omega^2}{(\omega-\omega_1)^2+\frac{\Gamma_1^2}{4}}\frac{\Gamma_2}{(\omega_2-2\omega)^2+\frac{\Gamma_2^2}{4}}. \tag{10}$$

This result demonstrates that the photoabsorption profile in the two-photon process differs substantially from the single-photon case. The cross section (10) has a resonance at the dipole plasmon frequency and, in addition, contains the quadrupole plasmon resonance at $\omega=\omega_2/2$.

The cross section (10) depends on $|z_{21}|^2$. The transition matrix element z_{21} describes the electron transition between the dipole and quadrupole plasmon resonance states. This is a single-electron transition rather than a collective one. Therefore, calculation of z_{21} on the basis of the sum rule (4)

would lead to a significant overestimate of the value of this matrix element. Instead, one can use Heisenberg's uncertainty principle for the evaluation of z_{21} [26]. By estimating the radial component of the momentum of a single electron in a dipole and quadrupole plasmon oscillatory mode as $p_1 \sim m\omega_1 \Delta R$ and $p_2 \sim m\omega_2 \Delta R$, respectively, one obtains

$$|z_{21}| \sim \min(\Delta z_1, \Delta z_2) \sim \frac{\hbar}{p_2} \sim A \frac{\hbar}{m\omega_1 \Delta R}. \tag{11}$$

Here, A is a dimensionless constant, of the order of one, $\Delta z_1 \sim \hbar/p_1$ and $\Delta z_2 \sim \hbar/p_2$ are the uncertainties relating to an electron in the dipole and quadrupole plasmon modes, respectively, ΔR is the width of the layer near the cluster surface within which plasmon excitations take place. In Appendix A we prove the correctness of this estimate and demonstrate that the matrix element

$$z_{21} = -\frac{8}{3}\left(\frac{6}{5}\right)^{1/4} \frac{\hbar}{m\omega_1 \Delta R}. \tag{12}$$

By substituting Eq. (12) in Eq. (10), we obtain the final expression for the two-photon absorption cross section,

$$\sigma_2 = \left(\frac{4\pi N e^2}{mc}\right)^2 \frac{A^2 \hbar}{2m\omega_1 N \Delta R^2} \frac{\omega^2}{\omega_1^2} \frac{1}{(\omega-\omega_1)^2 + \frac{\Gamma_1^2}{4}} \times \frac{\Gamma_2}{(\omega_2 - 2\omega)^2 + \frac{\Gamma_2^2}{4}}, \tag{13}$$

where $A = \frac{8}{3}(6/5)^{1/4} \approx 2.79$.

We note that the cross section (13) depends explicitly on Planck's constant $\hbar$, while the cross section (6) does not. The independence of Eq. (6) from $\hbar$ is connected with the fact that plasmon oscillations are a purely classical effect, while the dependence of Eq. (13) on $\hbar$ arises from the interaction between dipole and quadrupole plasmon modes as can be seen from estimate (11) and the explicit expression (12). This indicates that it is meaningful to treat plasmon excitations classically, while the coupling of various plasmon modes in the multiphoton photoabsorption process must be treated beyond purely classical theory.

In Fig. 1 we plot the cross section profiles per unit atom for single-photon (dashed line) and two-photon (solid line) absorption calculated according to Eqs. (6) and (13). These profiles do not depend on the number of atoms in the cluster. Note that the scales are not the same for the two curves for reasons of definition of the cross sections in the single- and two-photon cases, but both are given in atomic units. The peak in the single-photon plot gives the location of the dipole resonance. The other peak in the two-photon plot is the quadrupole resonance. This figure demonstrates a significant difference between the nature of the profiles, arising from the presence of quadrupole plasmon excitation in the two-photon case. In this calculation we have input $r_0 = 4.0$ and $\Gamma_1 = \omega_1/4$, $\Gamma_2 = \omega_2/4$, $\Delta R = r_0$. The choice of these parameters can be different for different clusters, but it should always lead to qualitatively similar single- and two-photon absorption profiles. An accurate determination of the parameters is only possible on the basis of *ab initio* calculations.

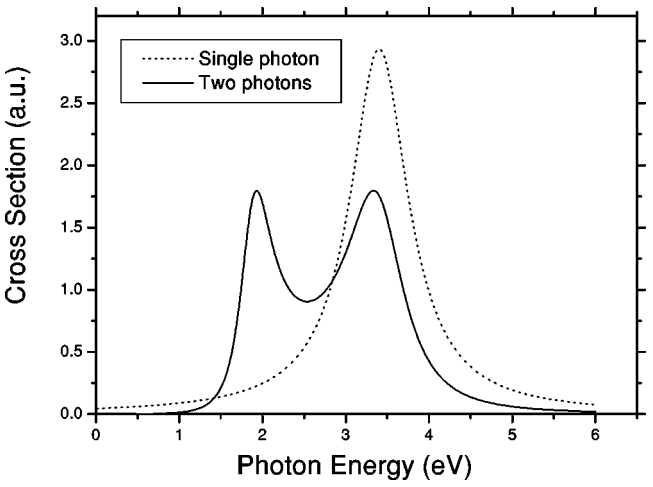

FIG. 1. The profiles of single-photon (dotted line) and two-photon (solid line) absorption calculated according to Eqs. (6) and (13) and normalized per unit atom. The two-photon absorption profile is scaled by a factor 1/100. The scales are not identical for the two curves for reasons of definition of the cross sections in the single- and two-photon cases, but both are given in atomic units.

C. *n*-photon absorption

The formalism we have developed can also be used for the evaluation of the multiphoton absorption cross sections for a larger number of photons. In the dipole approximation the *n*-photon absorption cross section has the following form:

$$\sigma_n = \frac{(2\pi)^{n+1} n!^2 e^{2n} \hbar^{n-1}}{c^n} \omega^n \sum_k |M_k|^2 \delta(\omega_{ko} - n\hbar\omega). \tag{14}$$

Here the amplitude M_n is equal to

$$M_k = \sum_{m_{n-1}} \sum_{m_{n-2}} \cdots \sum_{m_1} \frac{z_{km_{n-1}}}{[(n-1)\hbar\omega - \omega_{m_{n-1}0} + i\delta]} \times \frac{z_{m_{n-1}m_{n-2}}}{[(n-2)\hbar\omega - \omega_{m_{n-2}0} + i\delta]} \cdots \frac{z_{m_1 0}}{(\hbar\omega - \omega_{m_1 0} + i\delta)}. \tag{15}$$

The plasmon resonance structure of the multiphoton absorption cross section (15) can be analyzed in a way similar to the previous treatments for the single- and two-photon cases. This analysis immediately leads to the important conclusion that plasmon resonances with larger angular momenta (octupole, etc.) can be excited in the multiphoton absorption regime. Thus, for example, with three photons, the octupole plasmon resonance at $\omega = \omega_3/3$ will also be excited.

This analysis, however, leaves undefined the matrix elements for electronic transitions between various plasmon modes. Estimates of these can be performed either on the basis of Heisenberg's uncertainty principle or by a calculation similar to the one for Z_{12} [see Eqs. (12) and (10)] in the two-photon case, but their accurate evaluation is not trivial.

Note that the plasmon resonance approximation allows one to analyze only the plasmon resonance excitations that are characterized by relatively low angular momenta, because electron excitations in the cluster with large angular momenta l have single-particle character. This follows, for instance, from the fact that with increasing l the wavelength of the surface plasmon mode, $2\pi R/l$, becomes smaller than the characteristic wavelength of the delocalized electrons at the Fermi surface, $2\pi\hbar/\sqrt{2m\Delta\varepsilon}$, where $\Delta\varepsilon$ is the characteristic electron excitation energy in the cluster. In other words, excitations with angular momenta comparable with the characteristic electron angular momenta of the ground state exhibit single-particle rather than collective character. Therefore, when analyzing contributions of the plasmon resonance modes to the multiphoton absorption cross section, one should consider only the lowest angular momenta. For example, according to the jellium model, the maximum angular momentum of the delocalized electrons in the Na_{40} cluster is equal to 4. Therefore, only dipole and quadrupole collective modes can be expected in this case. With increasing cluster size the number of essential plasmon modes grows as R.

III. HYDRODYNAMIC DESCRIPTION OF COLLECTIVE MOTION OF THE ELECTRON DENSITY IN A CLUSTER

The multipole plasmon resonances arising in the multiphoton absorption cross sections should also appear in other physical characteristics of the cluster, which can be probed in the multiphoton absorption regime. In the situation where plasmon resonance excitations are the dominant contribution to the multiphoton absorption cross section, it is natural to seek and analyze the plasmon resonance structure of the variation of electron density induced by the radiation field. The variation of electron density is a characteristic of the system, allowing one easily to connect classical and quantum descriptions of the excitation process, because charge-density variation has the same meaning in both quantum and classical mechanics. A classical description of the electron-density variation in a cluster is appropriate in the situation where plasmon excitations dominate over the single-particle spectrum, because plasmon oscillations in clusters are an essentially classical effect.

A. Basic equations

Since our object of interest is the excitation of plasmons in metallic clusters, which have a distinctly classical nature, we now describe the collective motion of the electron density using Euler's equation and the equation of continuity.

Euler's equation couples the acceleration of the electron density $d\mathbf{v}/dt$ with the total local electric field $\mathbf{E}$ acting on the density at the point $(\mathbf{r},t)$. It has the following form:

$$\frac{d\mathbf{v}(\mathbf{r},t)}{dt}=\frac{e}{m}\mathbf{E}(\mathbf{r},t). \tag{16}$$

The electric field $\mathbf{E}$ includes both the external field acting on the cluster and the polarization contribution arising from the variation of electron density. Expressing the total derivative on the left-hand side of Eq. (16) as the sum of two contributions, arising from the change in velocity of the electron density in time and in space, one obtains

$$\frac{\partial\mathbf{v}(\mathbf{r},t)}{\partial t}+\{\mathbf{v}(\mathbf{r},t)\cdot\boldsymbol{\nabla}\}\cdot\mathbf{v}(\mathbf{r},t)$$

$$=-\frac{e}{m}\boldsymbol{\nabla}\varphi(\mathbf{r},t)-\frac{e}{m}\boldsymbol{\nabla}\int d\mathbf{r}'\frac{\delta\rho(\mathbf{r}',t)}{|\mathbf{r}-\mathbf{r}'|}. \tag{17}$$

Here $\varphi(\mathbf{r},t)$ is the potential of the external field. The second term on the right-hand side of Eq. (17) describes the polarization force due to the variation of electron density $\delta\rho(\mathbf{r},t)$.

We assume that the external potential $\varphi(\mathbf{r},t)$ is the solution of the wave equation. Therefore, we can put

$$\varphi(\mathbf{r},t)=e^{i\omega t}\varphi(\mathbf{r}), \tag{18}$$

where $\varphi(\mathbf{r},t)$ satisfies the equation

$$\Delta\varphi(\mathbf{r})=-k^2\varphi(\mathbf{r}). \tag{19}$$

Here $k=\omega/c$, c is the velocity of light, but in principle one can postulate a more complex dispersion law. We need consider only the positive frequency solution of the wave equation, because the formalism for the negative frequency solution is analogous to it.

The total electron density in the cluster is

$$\rho(\mathbf{r},t)=\rho_o(\mathbf{r})+\delta\rho(\mathbf{r},t), \tag{20}$$

where $\rho_o(\mathbf{r})$ is the electron-density distribution in a free cluster without an external field and $\delta\rho(\mathbf{r},t)$ is the variation of electron density caused by the external field and the polarization force acting together.

The motion of electron density in the cluster obeys the equation of continuity, which reads

$$\frac{\partial\rho(\mathbf{r},t)}{\partial t}+\boldsymbol{\nabla}\cdot\{\rho(\mathbf{r},t)\mathbf{v}(\mathbf{r},t)\}=0. \tag{21}$$

The simultaneous solution of Eqs. (17), (20), and (21) with appropriate initial conditions and the initial distribution $\rho_o(\mathbf{r})$ allow one to determine the variation of electron density $\delta\rho(\mathbf{r},t)$ as well as its velocity $\mathbf{v}(\mathbf{r},t)$. We solve this problem by using a perturbative approach on the external field $\varphi(\mathbf{r},t)$.

B. Perturbation theory

It is easy to estimate the relative value of the first and the second terms on the left-hand side of Eq. (17). We see that the second term is negligible, provided the condition E

$\ll m\omega^2 R/e$ is fulfilled. Substituting here the characteristic values $\omega \sim 0.1$, $R \sim 10$, one derives $E \ll 0.1$ in atomic units or $E \ll 5\times 10^8$ V/cm. Below, we assume that this condition is fulfilled and neglect the second term on the left-hand side of Eq. (17), which means physically that the external field causes only a small spatial inhomogeneity in the electron-density distribution within the cluster. In this limit, Euler's equation reduces to a Newtonian equation, which describes electronic motion in the cluster under the action of the external field and the polarization force.

We express the solutions of Eqs. (17) and (21) in the following form:

$$\delta\rho(\mathbf{r},t)=\sum_{n=1}^{\infty}\delta\rho_n(\mathbf{r})e^{in\omega t}, \tag{22}$$

$$\mathbf{v}(\mathbf{r},t)=\sum_{n=1}^{\infty}\mathbf{v}_n(\mathbf{r})e^{in\omega t}. \tag{23}$$

By substituting these expansions into Eqs. (17) and (21) and performing simple transformations, one derives

$$\mathbf{v}_n(\mathbf{r})=\frac{ie}{mn\omega}\delta_{n,1}\nabla\varphi(\mathbf{r})+\frac{ie}{mn\omega}\nabla\int d\mathbf{r}'\frac{\delta\rho_n(\mathbf{r}')}{|\mathbf{r}-\mathbf{r}'|}, \tag{24}$$

$$i\omega n\,\delta\rho_n(\mathbf{r})+\nabla\cdot\{\rho_0(\mathbf{r})\cdot\mathbf{v}_n(\mathbf{r})\}+\sum_{k'=1}^{n-1}\nabla\cdot\{\delta\rho_{k'}(\mathbf{r})\cdot\mathbf{v}_{n-k'}(\mathbf{r})\}=0. \tag{25}$$

Here $\delta_{n,1}$ is the Kroneker delta. One can exclude $\mathbf{v}_n(\mathbf{r})$ from Eq. (25) by the substitution of Eq. (24) in Eq. (25). Performing this transformation with the simultaneous use of Eq. (19) and $\Delta|\mathbf{r}-\mathbf{r}'|^{-1}=-4\pi\delta(\mathbf{r}-\mathbf{r}')$, one derives the following equation:

$$\left((\omega n)^2-\frac{4\pi e}{m}\rho_o(\mathbf{r})\right)\delta\rho_n(\mathbf{r})+\frac{e}{m}\nabla\rho_o(\mathbf{r})\cdot\nabla\int d\mathbf{r}'\frac{\delta\rho_n(\mathbf{r}')}{|\mathbf{r}-\mathbf{r}'|}$$
$$=\frac{e}{m}\delta_{n,1}[\rho_o(\mathbf{r})\varphi(\mathbf{r})k^2-\nabla\varphi(\mathbf{r})\cdot\nabla\rho_o(\mathbf{r})]+i\omega\sum_{k'=1}^{n-1}\nabla\cdot[\delta\rho_{k'}(\mathbf{r})\cdot\mathbf{v}_{n-k'}(\mathbf{r})]. \tag{26}$$

The left-hand side of Eq. (26) describes eigenoscillations of the electron density. The electron density is almost constant within the cluster but varies rapidly near the cluster surface. Therefore, the terms proportional to $\rho_o(\mathbf{r})$ and $\nabla\rho_o(\mathbf{r})$ on the left-hand side of Eq. (26) determine the square of the frequency of the volume and surface-plasmon oscillations, respectively. The right-hand side in Eq. (26) describes a driving force acting on the eigenplasmon oscillations.

The set of nonlinear equations (24) and (26) must be solved iteratively. It is clear from the form of the equations that the index n corresponds to the order of perturbation theory on the external field $\varphi(\mathbf{r})$.

Indeed, for $n=1$ Eq. (26) reduces to

$$\left(\omega^2-\frac{4\pi e}{m}\rho_o(\mathbf{r})\right)\delta\rho_1(\mathbf{r})+\frac{e}{m}\nabla\rho_o(\mathbf{r})\cdot\nabla\int d\mathbf{r}'\frac{\delta\rho_1(\mathbf{r}')}{|\mathbf{r}-\mathbf{r}'|}=\frac{e}{m}[\rho_o(\mathbf{r})\varphi(\mathbf{r})k^2-\nabla\varphi(\mathbf{r})\cdot\nabla\rho_o(\mathbf{r})] \tag{27}$$

and, for $n=2$, one derives

$$\left((2\omega)^2-\frac{4\pi e}{m}\rho_o(\mathbf{r})\right)\delta\rho_2(\mathbf{r})+\frac{e}{m}\nabla\rho_o(\mathbf{r})\cdot\nabla\int d\mathbf{r}'\frac{\delta\rho_2(\mathbf{r}')}{|\mathbf{r}-\mathbf{r}'|}=i\omega\nabla\cdot[\delta\rho_1(\mathbf{r})\mathbf{v}_1(\mathbf{r})]. \tag{28}$$

Equations (27) and (28) show that the variation $\rho_1(\mathbf{r}')$ describes the linear response of the electron subsystem to the the external field $\varphi(\mathbf{r})$, while $\rho_2(\mathbf{r}')$ arises only in the second order of perturbation theory on $\varphi(\mathbf{r})$, because $\rho_1(\mathbf{r}')\sim\varphi(\mathbf{r})$ and $\mathbf{v}_1(\mathbf{r})\sim\varphi(\mathbf{r})$.

Solving the set of equations (24) and (26) with $\varphi(\mathbf{r})$ describing the dipole electron-photon interaction up to the nth order, one can calculate the variation of electron density in the cluster caused by the field of n photons.

The set of equations (24) and (26) is not confined in its application to photons. It can also be used to describe the dynamics of electron density under the action of any kind of external field, for example, the electric field of a charged projectile colliding with the cluster. Indeed, by considering the partial spherical harmonic of the Fourier image of the Coulomb field of the projectile particle, one can derive from Eq. (27) the same expression for the variation of the electron density $\delta\rho_1(\mathbf{r})$, as follows from the purely electrodynamical perturbative approach to the electron-scattering problem [21].

C. Spherically symmetric case

Equations (24) and (26) are valid for an arbitrary shape of the initial distribution $\rho_o(\mathbf{r})$. In the spherical case, the angular parts in Eqs. (24) and (26) can be separated. Thus, the cross section for n-photon absorption can in principle be extracted for arbitrarily large n, although the calculations become more and more tedious the higher n is. Let us consider this formalism in more detail.

In the case of the spherically symmetric initial distribution, one can put $\rho_o(\mathbf{r})=\rho_0(r)$. This relationship allows one easily to exclude angular variables from Eq. (26). Using this relationship together with the partial expansion for $\delta\rho_n(\mathbf{r})$ and $\varphi(\mathbf{r})$,

$$\delta\rho_n(\mathbf{r})=\sum_{l=0}^{\infty}\sum_{m=-l}^{l}\delta\rho_{l,m}^n(r)Y_{l,m}(\mathbf{n}_r), \tag{29}$$

$$\varphi(\mathbf{r})=\sum_{l=0}^{\infty}\sum_{m=-l}^{l}\varphi_{l,m}(r)Y_{l,m}(\mathbf{n}_r), \tag{30}$$

one derives

$$\left((\omega n)^2-\frac{4\pi e}{m}\rho_o(r)\right)\delta\rho^n_{l,m}(r)$$
$$+\frac{4\pi e\rho_o'(r)}{m(2l+1)}\int dr' G_l(r,r')\delta\rho^n_{l,m}(r')$$
$$=\frac{e}{m}\delta_{n,1}[\rho_o(r)\varphi_{l,m}(r)k^2-\varphi'_{l,m}(r)\rho_o'(r)]$$
$$-\frac{e}{m}\sum_{j=1}^{n-1}\frac{1}{n-j}\int d\Omega_{\mathbf{n}_r}Y^*_{l,m}(\mathbf{n}_r)$$
$$\times\left\{\nabla\delta\rho_j(\mathbf{r})\cdot\nabla\left(\delta_{n-j,1}\varphi(\mathbf{r})+\int d\mathbf{r}'\frac{\delta\rho_{n-j}(\mathbf{r}')}{|\mathbf{r}-\mathbf{r}'|}\right)\right.$$
$$\left.-\delta\rho_j(\mathbf{r})[\delta_{n-j,1}\varphi(\mathbf{r})k^2+4\pi\delta\rho_{n-j}(\mathbf{r})]\right\}. \quad (31)$$

Here, $Y_{l,m}(\mathbf{n}_r)$ is the spherical harmonic corresponding to the angular momentum l and the projection of the angular momentum m. When deriving Eq. (31), we have multiplied both sides of Eq. (26) by the spherical harmonic $Y^*_{l,m}(\mathbf{n}_r)$ and then integrated over $d\Omega_{\mathbf{n}_r}$. We also used the well-known expansion (see, e.g., Ref. [27])

$$\frac{1}{|\mathbf{r}-\mathbf{r}'|}=\frac{4\pi}{2l+1}\sum_{l=0}^{\infty}\sum_{m=-l}^{l}B_l(r,r')Y_{l,m}(\mathbf{n}_r)Y^*_{l,m}(\mathbf{n}'_r), \quad (32)$$

where function $B_l(r,r')$ is defined as follows:

$$B_l(r,r')=\frac{r^l}{r'^{l+1}}\Theta(r'-r)+\frac{r'^l}{r^{l+1}}\Theta(r-r'). \quad (33)$$

Here $\Theta(r'-r)$ is the step function. In Eq. (31) we have introduced the function $G_l(r,r')$, which is of the form

$$G_l(r,r')=r'^2\frac{\partial B_l(r,r')}{\partial r}=l\frac{r^{l-1}}{r'^{l-1}}\Theta(r'-r)$$
$$-(l+1)\frac{r'^{l+2}}{r^{l+2}}\Theta(r-r'). \quad (34)$$

When deriving Eq. (31), we have also made obvious transformations of the sum over k' on the right-hand side of Eq. (26) using Eqs. (19) and (24). Note that the sum over j in Eq. (31) still contains the integrals over the angular variables. The integration over the angular variables in the sum is straightforward, but somewhat cumbersome. It is also clear that the nongradient terms in the sum contain the integration of the product of three spherical harmonics, if one expands $\delta\rho_{n-j}(\mathbf{r})$ and $\varphi(\mathbf{r})$ according to Eqs. (29) and (30), which we denote as

$$I_1(l,m|l_1,m_1,|l_2,m_2)=\int d\Omega_{\mathbf{n}_r}Y^*_{l,m}(\mathbf{n}_r)Y_{l_1,m_1}(\mathbf{n}_r)$$
$$\times Y_{l_2,m_2}(\mathbf{n}_r). \quad (35)$$

The gradient terms in the sum contain the integration of a spherical harmonic multiplied by the scalar product of the two vector spherical harmonics,

$$I_2(l,m|l_1,m_1,|l_2,m_2)=\sqrt{l_1(l_1+1)l_2(l_2+1)}\int d\Omega_{\mathbf{n}_r}$$
$$\times Y^*_{l,m}(\mathbf{n}_r)\mathbf{Y}^{(1)}_{l_1,m_1}(\mathbf{n}_r)\cdot\mathbf{Y}^{(1)}_{l_2,m_2}\cdot(\mathbf{n}_r). \quad (36)$$

This type of integral arises, when one expresses the gradients of the potential and the density according to (see, e.g., Ref. [27])

$$\nabla\delta\rho^j_{l_1,m_1}(r)Y_{l_1,m_1}(\mathbf{n}_r)=\delta\rho^{j'}_{l_1,m_1}(r)\mathbf{Y}^{(-1)}_{l_1,m_1}(\mathbf{n}_r)$$
$$+\sqrt{l_1(l_1+1)}\frac{1}{r}\delta\rho^j_{l_1,m_1}(r)$$
$$\times\mathbf{Y}^{(1)}_{l_1,m_1}(\mathbf{n}_r), \quad (37)$$

$$\nabla\Phi^{n-j}_{l_2,m_2}(r)Y_{l_2,m_2}(\mathbf{n}_r)=\Phi^{(n-j)'}_{l_2,m_2}(r)\mathbf{Y}^{(-1)}_{l_2,m_2}(\mathbf{n}_r)$$
$$+\sqrt{l_2(l_2+1)}\frac{1}{r}\Phi^{(n-j)}_{l_2,m_2}(r)$$
$$\times\mathbf{Y}^{(1)}_{l_2,m_2}(\mathbf{n}_r). \quad (38)$$

Here $\mathbf{Y}^{(-1)}_{l,m}(\mathbf{n}_r)$, $\mathbf{Y}^{(1)}_{l,m}(\mathbf{n}_r)$ are, respectively, the longitudinal and the transverse vector spherical harmonics, the definition of which one can find in Ref. [27]. We mention some properties of these vector harmonics: $\mathbf{Y}^{(-1)}_{l,m}(\mathbf{n}_r)=\mathbf{n}_rY_{l,m}(\mathbf{n}_r)$, $\mathbf{Y}^{(1)}_{l,m}(\mathbf{n}_r)=\nabla_\Omega Y_{l,m}(\mathbf{n}_r)/\sqrt{l(l+1)}$, and $\mathbf{Y}^{(-1)}_{l,m}(\mathbf{n}_r)\cdot\mathbf{Y}^{(1)}_{l,m}(\mathbf{n}_r)=0$.

The potential $\Phi^{n-j}_{l_2,m_2}(r)$ in Eq. (38) is as follows:

$$\Phi^{n-j}_{l_2,m_2}(r)=\delta_{n-j,1}\varphi_{l_2,m_2}(r)$$
$$+\frac{4\pi}{(2l_2+1)}\int dr'r'^2B_l(r,r')\delta\rho^{n-j}_{l_2,m_2}(r'). \quad (39)$$

Since the explicit expressions for $I_1(l,m|l_1,m_1,|l_2,m_2)$ and $I_2(l,m|l_1,m_1,|l_2,m_2)$ are somewhat lengthy, they are presented in Appendix B.

Using the formulas written above, one can easily rewrite Eq. (31) in the following form:

$$\left((\omega n)^2-\frac{4\pi e}{m}\rho_o(r)\right)\delta\rho^n_{l,m}(r)+\frac{4\pi e\rho_o'(r)}{m(2l+1)}\int dr' G_l(r,r')\delta\rho^n_{l,m}(r')$$

$$=\frac{e}{m}\delta_{n,1}(\rho_o(r)\varphi_{l,m}(r)k^2-\varphi'_{l,m}(r)\rho_o'(r))-\frac{e}{m}\sum_{j=1}^{n-1}\frac{1}{n-j}\sum_{\substack{l_1,m_1\\ l_2,m_2}} I_1(l,m|l_1,m_1,|l_2,m_2)\{\delta\rho^{j'}_{l_1,m_1}(r)\Phi^{(n-j)'}_{l_2,m_2}(r)$$

$$-\delta\rho^j_{l_1,m_1}(r)[\delta_{n-j,1}\varphi_{l_2,m_2}(r)k^2+4\pi\delta\rho^{n-j}_{l_2,m_2}(r)]\}-\frac{e}{mr^2}\sum_{j=1}^{n-1}\frac{1}{n-j}\sum_{\substack{l_1,m_1\\ l_2,m_2}} I_2(l,m|l_1,m_1,|l_2,m_2)\delta\rho^j_{l_1,m_1}(r)\Phi^{n-j}_{l_2,m_2}(r). \tag{40}$$

Here and below, we assume that the summation over l_1,m_1 and l_2,m_2 is performed with the same limits as in Eqs. (29) and (30).

D. Surface and volume plasmons

We now analyze Eq. (40) and demonstrate that it describes both surface- and volume-plasmon oscillations. The surface and volume solutions of Eq. (40) can be separated from each other, if one assumes that the initial distribution of electron density has the form

$$\rho_o(r)=\frac{Ne}{V}\Theta(R_v-r). \tag{41}$$

Here N is the total number of delocalized electrons in the cluster volume $V=4\pi R_v^3/3$.

In this case it is natural to look for the solution of Eq. (40) by expressing it in the following form:

$$\delta\rho^n_{l,m}(r)=\delta\rho^{s(n)}_{l,m}\delta(R_s-r)+\delta\rho^{v(n)}_{l,m}(r)\Theta(R_v-r). \tag{42}$$

In Eqs. (41) and (42) we have introduced the two radii R_v and R_s and assumed that $R_v<R_s=R$, but $R_v\to R_s=R$, where R is the cluster radius. Such a relationship is necessary for the elimination of the uncertainties, which arise in Eq. (42) and the subsequent formulas around the cluster radius. Physically, it means that surface and volume plasmons are defined in different parts of the space. In another words, by definition, the surface charge density should not be present inside the volume and vice versa.

Substituting Eqs. (41) and (42) in Eq. (40), performing straightforward but lengthy calculations of the integrals, one derives the following equation:

$$[(\omega n)^2-\omega_p^2]\delta\rho^{v(n)}_{l,m}(r)\Theta(R-r)+[(\omega n)^2-\omega_l^2]\delta\rho^{s(n)}_{l,m}\delta(R-r)$$

$$=-\frac{4\pi e^2N(l+1)}{m(2l+1)VR^{l+2}}\delta(R-r)\int_0^R dr' r'^{l+2}\delta\rho^{v(n)}_{l,m}(r')+\frac{Ne^2}{mV}\delta_{n,1}\varphi_{l,m}(r)k^2\Theta(R-r)+\frac{Ne^2}{mV}\delta_{n,1}\varphi'_{l,m}(R)\delta(R-r)$$

$$+\frac{e}{m}\delta(R-r)\sum_{j=1}^{n-1}\frac{1}{n-j}\sum_{\substack{l_1,m_1\\ l_2,m_2}} I_1(l,m|l_1,m_1,|l_2,m_2)\{\delta\rho^{s(j)}_{l_1,m_1}\tilde\Phi^{(n-j)''}_{l_2,m_2}(R)+\delta\rho^{v(j)}_{l_1,m_1}(R)\Phi^{(n-j)'}_{l_2,m_2}(R)$$

$$+\delta_{n-j,1}k^2\delta\rho^{s(j)}_{l_1,m_1}\varphi_{l_2,m_2}(R)\}-\frac{e}{m}\Theta(R-r)\sum_{j=1}^{n-1}\frac{1}{n-j}\sum_{\substack{l_1,m_1\\ l_2,m_2}} I_1(l,m|l_1,m_1,|l_2,m_2)\{\delta\rho^{v(j)'}_{l_1,m_1}(r)\Phi^{(n-j)'}_{l_2,m_2}(r)$$

$$-\delta\rho^{v(j)}_{l_1,m_1}(r)[\delta_{n-j,1}k^2\varphi_{l_2,m_2}(r)-4\pi\delta\rho^{v(j)}_{l_2,m_2}(r)]\}-\frac{e}{mR^2}\delta(R-r)\sum_{j=1}^{n-1}\frac{1}{n-j}\sum_{\substack{l_1,m_1\\ l_2,m_2}} I_2(l,m|l_1,m_1,|l_2,m_2)$$

$$\times\delta\rho^{s(j)}_{l_1,m_1}\Phi^{(n-j)}_{l_2,m_2}(R)-\frac{e}{mr^2}\Theta(R-r)\sum_{j=1}^{n-1}\frac{1}{n-j}\sum_{\substack{l_1,m_1\\ l_2,m_2}} I_2(l,m|l_1,m_1,|l_2,m_2)\delta\rho^{v(j)}_{l_1,m_1}(r)\Phi^{(n-j)}_{l_2,m_2}(r). \tag{43}$$

When deriving Eq. (43), we have used the fact that $\Theta'(R-r)=-\delta(R-r)$. Also we have introduced the functions

$$\Phi^{n-j}_{l_2,m_2}(r)=\delta_{n-j,1}\varphi_{l_2,m_2}(r)+\frac{4\pi}{(2l_2+1)}\int_0^R dr' r'^2 B_{l_2}(r,r') \times \delta\rho^{v(n-j)}_{l_2,m_2}(r')+\frac{4\pi R^2}{(2l_2+1)}\delta\rho^{s(n-j)}_{l_2,m_2}B_{l_2}(r,R),$$

$$\Phi^{(n-j)'}_{l_2,m_2}(r)=\delta_{n-j,1}\varphi'_{l_2,m_2}(r)+\frac{4\pi}{(2l_2+1)}\int_0^R dr' G_{l_2}(r,r') \times \delta\rho^{v(n-j)}_{l_2,m_2}(r')+\frac{4\pi}{(2l_2+1)}\delta\rho^{s(n-j)}_{l_2,m_2}G_{l_2}(r,R),$$

$$\Phi^{(n-j)''}_{l_2,m_2}(r)=\delta_{n-j,1}\varphi''_{l_2,m_2}(r)+\frac{4\pi}{(2l_2+1)}\int_0^R dr' D_{l_2}(r,r') \times \delta\rho^{v(n-j)}_{l_2,m_2}(r')-4\pi\delta\rho^{v(n-j)}_{l_2,m_2}(r)+\frac{4\pi}{(2l_2+1)} \times \delta\rho^{s(n-j)}_{l_2,m_2}D_{l_2}(r,R)-4\pi\delta\rho^{s(n-j)}_{l_2,m_2}\delta(R-r) =\tilde{\Phi}^{(n-j)''}_{l_2,m_2}(r)-4\pi\delta\rho^{s(n-j)}_{l_2,m_2}\delta(R-r),$$

$$D_l(r,r')=l_2(l_2-1)\frac{r^{l_2-2}}{r'^{l_2-1}}\Theta(r'-r)+(l_2+1)(l_2+2)\frac{r'^{l_2+2}}{r^{l+3}}\Theta(r-r'). \quad (44)$$

The physical origin of three terms in $\Phi^{n-j}_{l_2,m_2}(r)$ is clear. The first term describes the potential of the external field. The second term is the potential created by variation of the volume charge density. The third term is the potential created by the surface charge. The potential $\Phi^{n-j}_{l_2,m_2}(r)$ is continuous at the cluster surface, $B_{l_2}(R,R)=1/R$, $G_{l_2}(R,R)=0$, $D_{l_2}(R,R)=0$, $\delta\rho^{v(n-j)}_{l_2,m_2}(R)=0$.

The left-hand side of Eq. (43) describes volume and surface eigenoscillations of the electron density characterized by the angular momentum l. The surface-plasmon resonance frequency ω_l is the same as in Eq. (2). The volume-plasmon resonance frequency is equal to

$$\omega_p=\sqrt{\frac{4\pi e^2 N}{mV}}. \quad (45)$$

In Eq. (43), ω_p appears in expressions involving l, but is nevertheless independent of l, as one sees in Eq. (45). The physical reason for this is that the volume-plasmon oscillation is degenerate with l. The right-hand side of Eq. (43) describes a driving force acting on the eigenplasmon oscillations.

Surface and volume terms on the right-hand side of Eq. (43) have not been regrouped, in order to stress their correspondence with terms in Eq. (40). It is seen from Eq. (43) that equations for the volume- and surface-plasmon oscillations can be separated and will then read as follows:

$$[(\omega n)^2-\omega_p^2]\delta\rho^{v(n)}_{l,m}(r)=\frac{Ne^2}{mV}\delta_{n,1}\varphi_{l,m}(r)k^2-\frac{e}{m}\sum_{j=1}^{n-1}\frac{1}{n-j}\sum_{\substack{l_1,m_1\\ l_2,m_2}} I_1(l,m|l_1,m_1,|l_2,m_2)\{\delta\rho^{v(j)'}_{l_1,m_1}(r)\Phi^{(n-j)'}_{l_2,m_2}(r)-\delta\rho^{v(j)}_{l_1,m_1}(r) \times[\delta_{n-j,1}k^2\varphi_{l_2,m_2}(r)-4\pi\delta\rho^{v(j)}_{l_2,m_2}(r)]\}-\frac{e}{mr^2}\sum_{j=1}^{n-1}\frac{1}{n-j}\sum_{\substack{l_1,m_1\\ l_2,m_2}} I_2(l,m|l_1,m_1,|l_2,m_2) \times\delta\rho^{v(j)}_{l_1,m_1}(r)\Phi^{(n-j)}_{l_2,m_2}(r), \quad (46)$$

$$[(\omega n)^2-\omega_l^2]\delta\rho^{s(n)}_{l,m}=\frac{Ne^2}{mV}\delta_{n,1}\varphi'_{l,m}(R)-\frac{4\pi e^2 N(l+1)}{m(2l+1)VR^{l+2}}\int_0^R dr' r'^{l+2}\delta\rho^{v(n)}_{l,m}(r')+\frac{e}{m}\sum_{j=1}^{n-1}\frac{1}{n-j}\sum_{\substack{l_1,m_1\\ l_2,m_2}} I_1(l,m|l_1,m_1,|l_2,m_2) \times\{\delta\rho^{s(j)}_{l_1,m_1}\tilde{\Phi}^{(n-j)''}_{l_2,m_2}(R)+\delta\rho^{v(j)}_{l_1,m_1}(R)\Phi^{(n-j)'}_{l_2,m_2}(R)+\delta_{n-j,1}k^2\delta\rho^{s(j)}_{l_1,m_1}\varphi_{l_2,m_2}(R)\} -\frac{e}{mR^2}\sum_{j=1}^{n-1}\frac{1}{n-j}\sum_{\substack{l_1,m_1\\ l_2,m_2}} I_2(l,m|l_1,m_1,|l_2,m_2)\delta\rho^{s(j)}_{l_1,m_1}\Phi^{(n-j)}_{l_2,m_2}(R). \quad (47)$$

The set of nonlinear equations (46) and (47) must be solved iteratively starting from $n=1$. It is clear from the form of these equations that the index n corresponds to the order of perturbation theory on the external field $\varphi(\mathbf{r})$. It is also seen that the chain of equations for the volume-plasmon oscillations is self-sufficient, while the solutions for the surface oscillations also depend on those for volume, which is physically clear, because the electric field caused by volume oscillations of electron density must influence surface oscillations.

From Eqs. (46) and (47), one derives the following solutions for $n=1$:

$$\delta\rho_{l,m}^{v(1)}(r)=\frac{\omega_p^2}{4\pi}\frac{k^2\varphi_{l,m}(r)}{\omega^2-\omega_p^2}, \tag{48}$$

$$\delta\rho_{l,m}^{s(1)}=\frac{\omega_p^2}{4\pi}\frac{1}{\omega^2-\omega_l^2}\left\{\varphi'_{l,m}(R)-\frac{4\pi(l+1)}{(2l+1)}\int_0^R dr'\frac{r'^{l+2}}{R^{l+2}}\delta\rho_{lm}^{v(1)}(r')\right\}. \tag{49}$$

These equations show that, if the external field (30) is characterized by a certain angular momentum l_o and its projection m_o, i.e., $\varphi_{l,m}(r)=\delta_{l,l_o}\delta_{m,m_o}\varphi_{l_o,m_o}(r)$, then $\delta\rho_{l,m}^{s(1)}=\delta_{l,l_o}\delta_{m,m_o}\delta\rho_{l_o,m_o}^{s(1)}$ and $\delta\rho_{lm}^{v(1)}(r)=\delta_{l,l_o}\delta_{m,m_o}\delta\rho_{l_o,m_o}^{v(1)}(r)$. Assuming these dependencies, the solutions of Eqs. (46) and (47) for $n=2$ read as

$$\begin{aligned}\delta\rho_{l,m}^{v(2)}(r)=&-\frac{e}{m[(2\omega)^2-\omega_p^2]}I_1(l,m|l_o,m_o,|l_o,m_o)\\&\times\{\delta\rho_{l_o,m_o}^{v(1)'}(r)\Phi_{l_o,m_o}^{(1)'}(r)-\delta\rho_{l_o,m_o}^{v(1)}(r)\\&\times[k^2\varphi_{l_o,m_0}(r)-4\pi\delta\rho_{l_o,m_o}^{v(1)}(r)]\}\\&-\frac{e}{mr^2[(2\omega)^2-\omega_p^2]}I_2(l,m|l_o,m_o,|l_o,m_o)\\&\times\delta\rho_{l_o,m_o}^{v(1)}(r)\Phi_{l_o,m_o}^{(1)}(r),\end{aligned} \tag{50}$$

$$\begin{aligned}\delta\rho_{l,m}^{s(2)}=&-\frac{4\pi e^2N(l+1)}{m(2l+1)VR^{l+2}[(2\omega)^2-\omega_l^2]}\int_0^R dr'r'^{l+2}\delta\rho_{l_o,m_o}^{v(1)}(r')+\frac{e}{m[(2\omega)^2-\omega_l^2]}I_1(l,m|l_o,m_o,|l_o,m_o)\\&\times\{\delta\rho_{l_o,m_o}^{s(1)}\tilde{\Phi}_{l_o,m_o}^{(1)''}(R)+\delta\rho_{l_o,m_o}^{v(1)}(R)\Phi_{l_o,m_o}^{(1)'}(R)+k^2\delta\rho_{l_o,m_o}^{s(1)}\varphi_{l_o,m_o}(R)\}\\&-\frac{e}{mR^2[(2\omega)^2-\omega_l^2]}I_2(l,m|l_o,m_o,|l_o,m_o)\delta\rho_{l_o,m_o}^{s(1)}\Phi_{l_o,m_o}^{(1)}(r).\end{aligned} \tag{51}$$

By performing similar transformations, one can find the solutions $\delta\rho_{lm}^{v(n)}(r)$ and $\delta\rho_{lm}^{s(n)}$ for arbitrarily large n, although the formulas become more and more tedious the larger n becomes. These formulas demonstrate that, in the higher orders of perturbation theory, plasmon resonances with angular momenta larger than the angular momentum of the external field can be excited. Indeed, the selection rules for the integrals $I_1(l,m|l_o,m_o,|l_o,m_o)$ and $I_2(l,m|l_o,m_o,|l_o,m_o)$ (see Appendix B) show that the angular momentum in $\delta\rho_{lm}^{v(2)}(r)$ and $\delta\rho_{lm}^{s(2)}$ can be twice as large as l_o. Equations (46)–(51) also demonstrate that the plasmon resonances in $\delta\rho_{lm}^{v(n)}(r)$ and $\delta\rho_{lm}^{s(n)}$ arise when $\omega=\omega_p/n$ and $\omega=\omega_l/n$, respectively. These equations indicate a significant shift of the plasmon resonance profiles towards lower frequencies in the highest orders of perturbation theory.

These results have a simple physical explanation. Absorption of several quanta of the external field (photons) by the cluster leads to the excitation of nondipole plasmon oscillations of the electron density.

E. Fast electron-cluster collisions

Equations (46)–(51) can be used for the analysis of the balance between the surface- and volume-plasmon oscillations in the cluster. We demonstrate this for the example of fast electron scattering on a metal cluster. In this case, the external field of the projectile electron can be characterized by the Fourier component of the Coulomb potential

$$\varphi(r)=\frac{4\pi}{q^2}e^{i\mathbf{q}\cdot\mathbf{r}}, \tag{52}$$

where $\mathbf{q}=\mathbf{p}-\mathbf{p}'$ is the transferred momentum of the scattered electron.

The partial expansion of this potential reads as

$$\varphi(r)=4\pi\sum_{l=0}^{\infty}\sum_{m=-}^{m=l}i^l\varphi_{l,m}(r)Y_{l,m}^*(\mathbf{n}_q), \tag{53}$$

where the partial component of the potential

$$\varphi_{l,m}(r)=\frac{4\pi}{q^2}j_l(qr)Y_{l,m}(\mathbf{n}_r), \tag{54}$$

and $j_l(qr)$ is the spherical Bessel function (for definition see, e.g., Ref. [25]).

The form and properties of $\varphi_{l,m}(r)$, Eq. (54), are exactly the same as assumed in Eqs. (19) and (30). Therefore, from Eqs. (48) and (49), one can immediately derive

$$\delta\rho_{l,m}^{v(1)}(r)=\frac{\omega_p j_l(qr)}{\omega^2-\omega_p^2} \tag{55}$$

and

$$\delta\rho_{l,m}^{s(1)}=\frac{\omega_p}{q^2(\omega^2-\omega_l^2)}\left\{ j_l'(qR) - \frac{q^2\omega_p(l+1)}{(\omega^2-\omega_p^2)(2l+1)}\int_0^R dr'\frac{r'^{l+2}}{R^{l+2}}j_l(qr')\right\}. \tag{56}$$

In the case of inelastic electron scattering, ω has the meaning of the transferred energy in the collision, $\omega=\Delta\varepsilon=\varepsilon-\varepsilon'$. Calculating the integral in Eq. (56) with the use of the well-known properties of spherical Bessel functions (see, e.g., Ref. [25]), one derives

$$\delta\rho_{l,m}^{s(1)}=\frac{(2l+1)\omega_l^2}{\omega^2-\omega_l^2}\frac{j_l(qR)}{q^2R}-\frac{\omega_p^2}{\omega^2-\omega_p^2}j_{l+1}(qR). \tag{57}$$

Expressions (55) and (57) coincide with those calculated in Refs. [21,28] in the plasmon resonance approximation by purely electrodynamic means, as the response of a dielectric sphere, having dielectric permeability $\epsilon=1-\theta(R-r)\omega^2/\omega_p^2$.

From Eqs. (55) and (57), one can easily elaborate the electron inelastic scattering cross section in the plasmon resonance approximation, using the method described in Ref. [21],

$$\frac{d^2\sigma}{d\varepsilon' d\Omega}=\frac{4p'R}{\pi pq^4}\sum_l (2l+1)^2 j_l^2(qR)\frac{\omega_l^2\Delta\varepsilon\Gamma_l^s}{(\Delta\varepsilon^2-\omega_l^2)^2+\Delta\varepsilon^2\Gamma_l^{s2}} + \frac{2p'R^3}{\pi pq^2}\sum_l (2l+1)\frac{\omega_p^2\Delta\varepsilon\Gamma_l^v}{(\Delta\varepsilon^2-\omega_p^2)^2+\Delta\varepsilon^2\Gamma_l^{v2}} \times\left[j_l^2(qR)-j_{l+1}(qR)j_{l-1}(qR) -\frac{2}{qR}j_{l+1}(qR)j_l(qR)\right]. \tag{58}$$

This cross section is totally determined by collective electron excitations in the cluster. The first and the second terms in Eq. (58) describe the contributions of the surface- and the volume-plasmon excitations, respectively. In Eq. (58), we have also introduced widths, Γ_l^s and Γ_l^v, of the surface- and volume-plasmon resonances. They originate from the Landau damping mechanism of the plasmon excitations. For their determination we refer to the recent paper [21].

This result can be generalized to the cases, which are beyond the simple plasmon resonance approximation, by introducing the imaginary part of the cluster dynamic response function instead of using Lorentzian plasmon resonance profiles. The dynamic response function of a cluster can be either elaborated on the basis of the more advanced theoretical schemes or taken from experiment. Such an approach or a similar one has been utilized in a number of papers considering various aspects of electron collisions with metal clusters and small metal particles [28–30].

F. Multiphoton absorption

Next, we apply Eqs. (46) and (47) to the description of the multiphoton absorption process. In this paper, we focus our consideration on the analysis of plasmon excitations. If surface- or volume-plasmon resonances are excited by photons, i.e., $\omega\sim\omega_p$, then it is easy to check that the following condition is fulfilled $\omega R/c\sim\omega_p R/c\ll 1$, where c is the velocity of light. This condition implies the validity of the dipole approximation.

In the dipole approximation, one can neglect the momentum of the photon and put $k=0$. In this case, Eqs. (46) and (47) are simplified dramatically. Indeed, from Eq. (46), one derives

$$\delta\rho_{l,m}^{v(n)}(r)=0. \tag{59}$$

This result also simplifies Eq. (47) significantly for $\delta\rho_{lm}^{s(n)}$. After some trivial transformations it reduces to

$$[(\omega n)^2-\omega_l^2]\delta\rho_{l,m}^{s(n)}=\frac{Ne^2}{mV}\delta_{n,1}\varphi_{lm}'(R)++\frac{e}{m}\sum_{j=1}^{n-1}\frac{1}{n-j}\sum_{\substack{l_1,m_1\\ l_2,m_2}} I_1(l,m|l_1,m_1,|l_2,m_2)\delta\rho_{l_1,m_1}^{s(j)}\tilde{\Phi}_{l_2,m_2}^{(n-j)''}(R) - \frac{e}{mR^2}\sum_{j=1}^{n-1}\frac{1}{n-j}\sum_{\substack{l_1,m_1\\ l_2,m_2}} I_2(l,m|l_1,m_1,|l_2,m_2)\delta\rho_{l_1,m_1}^{s(j)}\Phi_{l_2,m_2}^{(n-j)}(R). \tag{60}$$

The partial component of the linearly polarized dipole photon field,

$$\varphi_{l,m}(r) = -\sqrt{\frac{4\pi}{3}} E r \delta_{l,1}\delta_{m,0}. \tag{61}$$

Here $E=\sqrt{2\pi\hbar\omega/V_o}$ is the strength of the photon's electric field and V_o is the normalization volume of the photon mode. Substituting Eq. (61) into Eq. (47) and using Eq. (44), one derives

$$[(\omega n)^2-\omega_l^2]\delta\rho_{l,m}^{s(n)} = -\sqrt{\frac{4\pi}{3}}\frac{Ne^2E}{mV}\delta_{n,1}\delta_{l,1}\delta_{m,0} + \sqrt{\frac{4\pi}{3}}\frac{eE}{mR}\sum_{l_1,m_1} I_2(l,m|l_1,m_1,|1,0)\,\delta\rho_{l_1,m_1}^{s(n-1)} - \frac{4\pi eE}{mR}\sum_{j_1=1}^{n-1}\frac{1}{n-j}\sum_{\substack{l_1,m_1\\ l_2,m_2}} I_2(l,m|l_1,m_1,|l_2,m_2)\frac{\delta\rho_{l_1,m_1}^{s(j)}\delta\rho_{l_2,m_2}^{s(n-j)}}{2l_2+1}. \tag{62}$$

This equation should be solved iteratively starting from $n=1$. For $n=1$, the single nontrivial solution, $\delta\rho_{1,0}^{s(1)}$, reads as

$$\delta\rho_{1,0}^{s(1)} = -\sqrt{\frac{4\pi}{3}}\frac{Ne^2E}{mV(\omega^2-\omega_1^2)}. \tag{63}$$

Then, for $n=2$, the solution of Eq. (62) is of the form

$$\delta\rho_{l,m}^{s(2)} = \sqrt{\frac{4\pi}{3}}\frac{e\,\delta\rho_{1,0}^{s(1)}\left(E-\sqrt{\frac{4\pi}{3}}\delta\rho_{1,0}^{s(1)}\right)}{mR[(2\omega)^2-\omega_l^2]} I_2(l,m|1,0|1,0). \tag{64}$$

The selection rules for $I_2(l,m|1,0|1,0)$ (see Appendix B) show that this integral does not vanish, when $l=0$ and $m=0$ or $l=2$ and $m=0$. Therefore, for $n=3$ from Eq. (62), one derives

$$\delta\rho_{l,m}^{s(3)} = \sqrt{\frac{4\pi}{3}}\frac{eE}{mR[(3\omega)^2-\omega_l^2]}\{I_2(l,m|0,0|1,0)\,\delta\rho_{0,0}^{s(2)} + I_2(l,m|2,0|1,0)\,\delta\rho_{2,0}^{s(2)}\} - \frac{4\pi eE\,\delta\rho_{1,0}^{s(1)}}{mR[(3\omega)^2-\omega_l^2]}\left\{\frac{5}{6}I_2(l,m|1,0|0,0)\,\delta\rho_{0,0}^{s(2)} + \frac{13}{30}I_2(l,m|2,0|1,0)\,\delta\rho_{2,0}^{s(2)}\right\}. \tag{65}$$

In Eq. (65), only the second terms in brackets give a nonzero contribution, since $I_2(l,m|0,0|1,0)=I_2(l,m|1,0|0,0)=0$ (see Appendix B). Substituting $\delta\rho_{1,0}^{s(1)}$ from Eq. (63) in Eq. (64) and $\delta\rho_{2,0}^{s(2)}$ from Eq. (64) in Eq. (65) and using the explicit expressions for the angular integrals given in Appendix B, one obtains

$$\delta\rho_{0,0}^{s(2)} = -\frac{\pi^{1/2}}{3m^2RV}\frac{Ne^3E^2}{(\omega^2-\omega_1^2)^2},$$

$$\delta\rho_{2,0}^{s(2)} = -\frac{4\pi^{1/2}}{3\sqrt{5}m^2RV}\frac{Ne^3E^2\omega^2}{(\omega^2-\omega_1^2)^2[(2\omega)^2-\omega_2^2]},$$

$$\delta\rho_{1,0}^{s(3)} = -\left(\frac{64\pi}{3}\right)^{1/2}\frac{16+3\sqrt{5}}{75m^3R^2V} \times\frac{Ne^4E^3\omega^2\left(\omega^2+\frac{3}{10}\omega_1^2\right)}{(\omega^2-\omega_1^2)^3[(2\omega)^2-\omega_2^2][(3\omega)^2-\omega_1^2]},$$

$$\delta\rho_{3,0}^{s(3)} = \left(\frac{4\pi}{7}\right)^{1/2}\frac{12(2+\sqrt{5})}{75m^3R^2V} \times\frac{Ne^4E^3\omega^2\left(\omega^2+\frac{3}{10}\omega_1^2\right)}{(\omega^2-\omega_1^2)^3[(2\omega)^2-\omega_2^2][(3\omega)^2-\omega_3^2]}. \tag{66}$$

IV. INDUCED MULTIPOLE MOMENTS IN THE CLUSTER

Let us now calculate the multipole moments of the cluster induced by an external radiation field on the basis of the model developed in the preceding section, and analyze their plasmon resonance structure.

The induced multipole moment of the cluster

$$Q_{l,m} = \sqrt{\frac{4\pi}{2l+1}}\int dV r^l Y_{l,m}(\mathbf{n}_r)\,\delta\rho(\mathbf{r}), \tag{67}$$

where the variation of electron density $\delta\rho(\mathbf{r})$ is determined in Eqs. (29) and (42). Subsituting Eqs. (29) and (42) in Eq. (67) and putting $\delta\rho_{l,m}^{v(n)}(r)=0$ for any n in the dipole approximation as follows from Eq. (59), one derives

$$Q_{l,m}^{(n)} = \sqrt{\frac{4\pi}{2l+1}}R^{l+2}\delta\rho_{l,m}^{s(n)}. \tag{68}$$

Substituting in Eq. (68) $\delta\rho_{1,0}^{s(n)}$ from Eq. (63), one obtains the expression for the dipole moment of the cluster induced in the single-photon absorption process,

$$D^{(1)}(\omega)=Q_{1,0}^{(1)}=-\frac{Ne^2E}{m(\omega^2-\omega_1^2+i\omega\Gamma_1)}. \tag{69}$$

The explicit expressions for the partial electron-density variations $\delta\rho_{l,m}^{s(n)}$ entering Eq. (68) for $n=2$ (two-photon case) and $n=3$ (three-photon case) are given in Eq. (66). Substituting the partial electron-density variations $\delta\rho_{0,0}^{s(2)}$ and $\delta\rho_{2,0}^{s(2)}$ from Eq. (66) into Eq. (68), one derives the expression for the monopole and quadrupole moment of the cluster induced in the two-photon regime,

$$M^{(2)}(\omega)=Q_{0,0}^{(2)}=-\frac{1}{2m^2R^2}\frac{Ne^3E^2}{[(\omega^2-\omega_1^2)^2+\omega^2\Gamma_1^2]},$$

$$Q^{(2)}(\omega)=Q_{2,0}^{(2)}=-\frac{2}{5}\frac{Ne^3E^2\omega^2}{m^2[(\omega^2-\omega_1^2)^2+\omega^2\Gamma_1^2][(2\omega)^2-\omega_2^2+i2\omega\Gamma_2]}. \tag{70}$$

Here, we have introduced the plasmon resonance widths Γ_1 and Γ_2 which take into account Landau damping of the dipole and quadrupole surface plasmon resonances. They must be determined separately, e.g., by an *ab initio* approach (see Ref. [21]).

By absorbing three photons one can induce dipole and octupole moments in the cluster. Substituting $\delta\rho_{1,0}^{s(3)}$ from Eq. (66) into Eq. (68), one derives the expression for the induced dipole moment,

$$D^{(3)}(\omega)=Q_{1,0}^{(3)}=-\frac{4(16+3\sqrt{5})}{75m^3R^2}\frac{Ne^4E^3\omega^2\left(\omega^2+\frac{3}{10}\omega_1^2\right)}{[(\omega^2-\omega_1^2)^2+\omega^2\Gamma_1^2](\omega^2-\omega_1^2+i\omega\Gamma_1)[(2\omega)^2-\omega_2^2+i2\omega\Gamma_2][(3\omega)^2-\omega_1^2+i3\omega\Gamma_1]}. \tag{71}$$

The expression for the octupole moment induced by three photons following from Eqs. (66) and (68) reads as

$$O^{(3)}(\omega)=Q_{3,0}^{(3)}=\frac{12(2+\sqrt{5})}{175m^3}\frac{Ne^4E^3\omega^2\left(\omega^2+\frac{3}{10}\omega_1^2\right)}{[(\omega^2-\omega_1^2)^2+\omega^2\Gamma_1^2](\omega^2-\omega_1^2+i\omega\Gamma_1)[(2\omega)^2-\omega_2^2+i2\omega\Gamma_2][(3\omega)^2-\omega_3^2+i3\omega\Gamma_3]}. \tag{72}$$

Here, we have also introduced the octupole plasmon resonance width Γ_3.

Expressions (69)–(72) demonstrate that the multipole moments induced in the cluster during multiphoton absorption processes possess a prominent plasmon resonance structure. The nature of these resonances is the same as occurs in the mutiphoton absorption cross sections discussed in Sec. II.

The connection between $D^{(1)}(\omega)$ from Eq. (69) and the cross section σ_1 found in Eq. (6) is straightforward,

$$\sigma_1=\frac{4\pi\omega}{cE}\,\mathrm{Im}\,D^{(1)}(\omega). \tag{73}$$

In the multiphoton regime, the connection between the induced multipole moments of the cluster and the multiphoton absorption cross section becomes more complex, which is apparent from the the classical nature of the expressions (70)–(72) and the explicit dependence of the multiphoton absorption cross sections on Planck's constant. The discussion of this interesting relationship is, however, beyond the scope of the present paper. We also note that the relationship between cross section of the photoabsorption process and the cluster dynamic response function similar to Eq. (73) provides a good way to improve the accuracy of the theoretical framework and to derive reliable qualitative results beyond the level of accuracy of the jellium model.

V. CONCLUSION

In this paper, we have developed a formalism that allows one to calculate the cross section for multiphoton absorption in the plasmon resonance approximation. We have demonstrated that plasmon excitations with angular momenta larger than 1 substantially alter the profile for multiphoton absorption as compared to the single-photon case.

Our model is formulated in terms of a charge-density distribution function $\rho(\mathbf{r})$ for the cluster. This means that, in principle, one can study the response for different charge-density profiles including deformed ones. Our model is a semiclassical one, which neglects the granularity of charge in the system. This is consistent with the principles underlying the jellium picture. It is appropriate for metallic clusters and, to a lesser extent, for fullerenes.

We have used the jellium framework for simplicity. In fact, all the conclusions regarding selection rules and the general behavior of single versus multiphoton cross sections are model independent. So, the jellium calculations are used in our work merely as an illustration of what happens when

the general formulas are applied.

In the classical formulation of our model, we have used Euler's equation for hydrodynamic flow, together with the equation of continuity. We have demonstrated that the results following from our model are consistent with direct estimates of the matrix elements for the multiphoton absorption process. The theoretical formalism we have developed is not confined in its application to photons. It can also be used to describe any kind of higher-order plasmon excitation processes, for example, those which arise by multiple scattering of electrons within a cluster.

ACKNOWLEDGMENTS

The authors acknowledge support from the Royal Society of London, INTAS, the DAAD, and the Alexander von Humboldt Foundation.

APPENDIX A: MATRIX ELEMENTS OF PLASMON RESONANCE TRANSITIONS

In this appendix, we evaluate the matrix elements of plasmon resonance transitions in the plasmon resonance approximation by the use of the sum rule.

For a stationary (i.e., explicitly independent of time) operator $\hat{F}$ of an observable physical quantity, characterizing a system of particles with the Hamiltonian $\hat{H}$, one can formulate the following sum rule (see, e.g., Ref. [25]):

$$\sum_n \omega_{n0}|\langle n|\hat{F}|0\rangle|^2=\frac{1}{2}\langle 0|[\hat{F},[\hat{H},\hat{F}]]|0\rangle. \tag{A1}$$

Here $\omega_{n0}=\varepsilon_n-\varepsilon_0$, the summation is performed over all excited states of the system and $[\hat{H},\hat{F}]$ denotes the commutator of the operators $\hat{H}$ and $\hat{F}$: $[\hat{H},\hat{F}]=\hat{H}\hat{F}-\hat{F}\hat{H}$.

Applying the sum rule (A1) to operator $\hat{F}$ defined as

$$\hat{F}=\sum_k F(\mathbf{r}_k), \tag{A2}$$

where $F(\mathbf{r}_k)$ is a function of the coordinates of the kth electron and the summation in Eq. (A2) is performed over all particles in the system, one derives

$$\sum_n \omega_{n0}|\langle n|\hat{F}|0\rangle|^2=\frac{\hbar^2}{2m}\int d\mathbf{r}|\boldsymbol{\nabla}F(\mathbf{r})|^2\rho(\mathbf{r}). \tag{A3}$$

Here $\rho(\mathbf{r})$ is the ground-state charge-density distribution in the system. Applying the general rule (A3) to the function

$$F(\mathbf{r})=\sqrt{\frac{4\pi}{2l+1}}r^l Y_{lm}(\mathbf{n}), \tag{A4}$$

and performing the integration in Eq. (A3) with the density distribution (41), one derives

$$\sum_n \omega_{n0}|\langle n|\hat{Q}_{lm}|0\rangle|^2=\frac{\hbar^2}{2}\omega_l^2 R^{2l+1}. \tag{A5}$$

Here, we have used the following definition of the multipole moments operator:

$$\hat{Q}_{lm}=\sqrt{\frac{4\pi}{2l+1}}\sum_{k=1}^{N} e_k r_k^l Y_{lm}(\mathbf{n}_k). \tag{A6}$$

The plasmon resonance frequencies in Eq. (A5) are defined according to Eq. (2).

Using Eq. (A5), one can easily evaluate the matrix elements of plasmon resonance transitions in the plasmon resonance approximation. Indeed, assuming that plasmon excitations dominate in the sum over n in Eq. (A5), one derives

$$Q_{lm}=\langle n|\hat{Q}_{lm}|0\rangle=\sqrt{\frac{\hbar\omega_l R^{2l+1}}{2}}=eR^{l-1}\sqrt{\frac{N\hbar}{2m\omega_l}}\sqrt{\frac{3l}{2l+1}}. \tag{A7}$$

Equation (A7) gives the matrix elements of plasmon resonance transitions for an arbitrary large angular momentum l. The correctness of the result (A7) can be independently verified by performing calculations of the multipole dynamic polarizability of the cluster in the plasmon resonance approximation. Indeed, using Eq. (A7), one derives

$$\alpha_l(\omega)=2\sum_n \frac{\omega_{n0}|Q_{l0}|^2}{\omega_{n0}^2-\omega^2-i\omega\Gamma_l}\approx\frac{R^{2l+1}\omega_l^2}{\omega_l^2-(\hbar\omega)^2-i\hbar^2\omega\Gamma_l}, \tag{A8}$$

which is the known expression for the dynamic multipole plasmon polarizability in the plasmon resonance approximation (see, e.g., Refs. [10,17]).

For the dipole plasmon resonance transition, one derives from Eq. (A7),

$$Q_{10}=d_{10}=ez_{10}=e\sqrt{\frac{N\hbar}{2m\omega_1}}, \tag{A9}$$

which is consistent with the dipole sum rule (4).

Equation (A7) allows one to evaluate the matrix elements of electronic transitions between various plasmon resonance states. To demonstrate this, let us rewrite Eq. (A7) in the form

$$Q_{lm}=\sqrt{\frac{1}{2l+1}}\int dr r^{l+2}\rho_{l0}(r). \tag{A10}$$

Here, we have introduced the radial transition density $\rho_{l0}(r)$ between the ground state and the excited plasmon resonance state with angular momentum l and used the relationship $I_1(l_n,m_n|l,m|0,0)=\delta_{l_n,l}\delta_{m_n,m}/\sqrt{4\pi}$, when calculating angular intergrals in Eq. (A10).

The radial transition density $\rho_{l0}(r)$ is localized near the cluster surface. Qualitatively, this is clear because $\rho_{l0}(r)$ describes the plasmon excitation. Quantitatively, this was proved by *ab initio* computations of the transition densities in the Na_{40} and Na_{92} clusters within the jellium model in Ref. [19]. Therefore, to a reasonable accuracy, one can approximate $\rho_{l0}(r)$ by the δ function,

$$\rho_{l0}(r)=\rho_{l0}\delta(r-R). \tag{A11}$$

Substituting Eq. (A11) into Eq. (A10) and comparing the result of the calculation with Eq. (A7), one can determine the value ρ_{l0} entering Eq. (A11). The result of this calculation reads as

$$\rho_{l0}=\frac{e}{R^3}\sqrt{\frac{3l\hbar N}{2m\omega_l}}. \tag{A12}$$

Let us now evaluate the matrix element for the dipole transition between plasmon resonance modes, which reads as

$$z_{l_2l_1}=\sqrt{\frac{4\pi}{3}}\int d\mathbf{r}Y_{1,0}(\mathbf{n})r\rho_{l_2l_1}(\mathbf{r}). \tag{A13}$$

Here, $\rho_{l_2l_1}(\mathbf{r})$ is the electron transition density between the dipole and the quadrupole plasmon modes. This transition density can be evaluated via the transition densities $\rho_{l_1,0}(r)$, $\rho_{l_2,0}(r)$ and the ground-state electron density of the cluster $\rho_{00}=eN/V$ as follows:

$$\rho_{l_2l_1}(\mathbf{r})=\frac{\rho_{l_20}(r)\rho_{l_10}(r)}{\rho_{00}}Y_{l_1,0}(\mathbf{n})Y_{l_2,0}(\mathbf{n}). \tag{A14}$$

Substituting Eq. (A14) into Eq. (A13) and performing simple transformations, one derives

$$z_{l_2l_1}=e\sqrt{\frac{4\pi l_1l_2}{3}}\left(\frac{l_1(2l_2+1)}{l_2(2l_1+1)}\right)^{1/4}\times I_1(l_2,m_2|1,0|l_1,m_1)\frac{2\pi\hbar}{m\omega_{l_1}}\delta(0). \tag{A15}$$

This equation has an uncertainty, which originates from the fact that we have assumed zero thickness for the layer near the cluster surface in which plasmon excitations take place. By introducing a finite width ΔR for this domain and using one of the standard representations of the δ function [25] to resolve the uncertainty, $\delta(0)\approx 2/\pi\Delta R$, one finally derives

$$z_{l_2l_1}=8e\sqrt{\frac{\pi l_1l_2}{3}}\left(\frac{l_1(2l_2+1)}{l_2(2l_1+1)}\right)^{1/4}\times I_1(l_2,m_2|1,0|l_1,m_1)\frac{\hbar}{m\omega_{l_1}\Delta R}. \tag{A16}$$

The explicit expression for the angular integral $I_1(l_2,m_2|1,0|l_1,m_1)$ is given in Appendix B. In the case of the transition between the dipole and quadrupole plasmon resonance states this integral is equal to $I_1(2,0|1,0|1,0)=-1/\sqrt{5\pi}$. Substituting this value into Eq. (A16) and performing simple algebraic transformations, one arrives at the expression for the matrix element describing the transition between the dipole and the quadrupole plasmon resonance modes,

$$z_{12}=-e\frac{8}{3}\left(\frac{6}{5}\right)^{1/4}\frac{\hbar}{m\omega_1\Delta R}. \tag{A17}$$

APPENDIX B: INTEGRALS $I_1(l,m|l_1,m_1,|l_2,m_2)$ AND $I_2(l,m|l_1,m_1,|l_2,m_2)$

The angular integral,

$$I_1(l,m|l_1,m_1|l_2,m_2)=\int d\Omega_{\mathbf{n}_r}Y^*_{l,m}(\mathbf{n}_r)Y_{l_1,m_1}(\mathbf{n}_r)Y_{l_2,m_2}(\mathbf{n}_r), \tag{B1}$$

is well known and can be found in many textbooks (see, e.g., Ref. [27]). It is equal to

$$I_1(l,m|l_1,m_1|l_2,m_2)=(-1)^m i^{l_1+l_2-l}\sqrt{\frac{(2l+1)(2l_1+1)(2l_2+1)}{4\pi}}\times\begin{pmatrix} l & l_1 & l_2\\ -m & m_1 & m_2\end{pmatrix}\begin{pmatrix} l & l_1 & l_2\\ 0 & 0 & 0\end{pmatrix}. \tag{B2}$$

Here, the integral is expressed via $3j$ symbols (for definition see, e.g., Ref. [27]).

The angular integral,

$$I_2(l,m|l_1,m_1|l_2,m_2)=\sqrt{l_1(l_1+1)l_2(l_2+1)}\times\int d\Omega_{\mathbf{n}_r}Y^*_{l,m}(\mathbf{n}_r)\mathbf{Y}^{(1)}_{l_1,m_1}(\mathbf{n}_r)\cdot\mathbf{Y}^{(1)}_{l_2,m_2}(\mathbf{n}_r), \tag{B3}$$

can be expressed via the sum of products of $3j$ symbols and $6j$ symbols (for definition see, e.g., Ref. [27]) after performing the following transformations.

Using the standard relationships for spherical vector harmonics, written in Ref. [27] on page 210, one derives

$$I_2(l,m|l_1,m_1|l_2,m_2)=\sqrt{l_1(l_1+1)l_2(l_2+1)}\int d\Omega_{\mathbf{n}_r}Y^*_{l,m}(\mathbf{n}_r)\times\left(\sqrt{\frac{l_1+1}{2l_1+1}}\mathbf{Y}^{l_1-1}_{l_1,m_1}(\mathbf{n}_r)+\sqrt{\frac{l_1}{2l_1+1}}\mathbf{Y}^{l_1+1}_{l_1,m_1}(\mathbf{n}_r)\right)\times\left(\sqrt{\frac{l_2+1}{2l_2+1}}\mathbf{Y}^{l_2-1}_{l_2,m_2}(\mathbf{n}_r)+\sqrt{\frac{l_2}{2l_2+1}}\mathbf{Y}^{l_2+1}_{l_2,m_1}(\mathbf{n}_r)\right). \tag{B4}$$

The integrations arising in Eq. (B4) can be performed and expressed via the sum of products of $3j$ symbols and $6j$ symbols, using the standard formulas given in Ref. [27] on pages 222 and 236. The result of the calculations of these integrals reads as

$$I_2(l,m|l_1,m_1|l_2,m_2)=(-1)^{l_1+l_2+l+m+1}\sqrt{l_1(l_1+1)l_2(l_2+1)(2l+1)}\begin{pmatrix} l_1 & l_2 & l \\ m_1 & m_2 & -m \end{pmatrix}$$
$$\times\Bigg\{\sqrt{\frac{(l_1+1)(l_2+1)(2l_1-1)(2l_2-1)}{4\pi}}\begin{pmatrix} l_1-1 & l_2-1 & l \\ 0 & 0 & 0 \end{pmatrix}\begin{Bmatrix} l_1-1 & l_2-1 & l \\ l_2 & l_1 & 1 \end{Bmatrix}$$
$$+\sqrt{\frac{l_1(l_2+1)(2l_1+3)(2l_2-1)}{4\pi}}\begin{pmatrix} l_1+1 & l_2-1 & l \\ 0 & 0 & 0 \end{pmatrix}\begin{Bmatrix} l_1+1 & l_2-1 & l \\ l_2 & l_1 & 1 \end{Bmatrix}$$
$$+\sqrt{\frac{(l_1+1)l_2(2l_1-1)(2l_2+3)}{4\pi}}\begin{pmatrix} l_1-1 & l_2+1 & l \\ 0 & 0 & 0 \end{pmatrix}\begin{Bmatrix} l_1-1 & l_2+1 & l \\ l_1 & l_2 & 1 \end{Bmatrix}$$
$$+\sqrt{\frac{l_1l_2(2l_1+3)(2l_2+3)}{4\pi}}\begin{pmatrix} l_1+1 & l_2+1 & l \\ 0 & 0 & 0 \end{pmatrix}\begin{Bmatrix} l_1+1 & l_2+1 & l \\ l_2 & l_1 & 1 \end{Bmatrix}\Bigg\}. \tag{B5}$$

For the particular cases of interest, one derives from Eq. (B5)

$$I_2(1,0|0,0|1,0)=0,\quad I_2(0,0|1,0|1,0)=\frac{1}{\sqrt{\pi}},\quad I_2(2,0|1,0|1,0)=\frac{1}{\sqrt{5\pi}},$$
$$I_2(1,0|2,0|1,0)=\frac{6}{10\sqrt{\pi}}\left(1+\frac{16}{3\sqrt{5}}\right),\quad I_2(3,0|2,0|1,0)=-\frac{18}{5\sqrt{105\pi}}\left(1+\frac{\sqrt{5}}{2}\right). \tag{B6}$$

[1] L. Köller, M. Schumacher, J. Köhn, S. Teuber, J. Tiggesbäumker, and K. H. Meiwes-Broer, Phys. Rev. Lett. **82**, 3783 (1999).

[2] C. A. Ullrich, P.-G. Reinhard, and E. Suraud, J. Phys. B **30**, 5043 (1997).

[3] S. Hunsche, T. Starczewski, A. l'Huillier, A. Persson, C-G. Wahlström, B. van Linden van der Heuvell, and S. Svanberg, Phys. Rev. Lett. **77**, 1966 (1996).

[4] W. A. de Heer, Rev. Mod. Phys. **65**, 611 (1993).

[5] M. Brack, Rev. Mod. Phys. **65**, 677 (1993).

[6] C. Brechignac and J. P. Connerade, J. Phys. B **27**, 3795 (1994).

[7] *Clusters of Atoms and Molecules, Theory, Experiment and Clusters of Atoms*, edited by H. Haberland, Springer Series in Chemical Physics Vol. 52 (Springer, New York, 1994).

[8] F. Alasia, R. A. Broglia, H. E. Roman, L. I. Serra, G. Colo, and J. M. Pacheco, J. Phys. B **27**, L663 (1994).

[9] M. Madjet, C. Guet, and W. R. Johnson, Phys. Rev. A **51**, 1327 (1995).

[10] U. Kreibig and M. Vollmer, *Optical Properties of Metal Clusters* (Springer-Verlag, Berlin, 1995).

[11] V. K. Ivanov, G. Yu. Kashenock, R. G. Polozkov, and A. V. Solov'yov, J. Phys. B **34**, L669 (2001).

[12] *Metal Clusters*, edited by W. Ekardt (Wiley, New York, 1999).

[13] A. V. Solov'yov, in *Electron Scattering on Metal Clusters and Fullerenes*, in NATO Advanced Study Institute, Proceedings of Les Houches Summer School Session LXXIII, edited by C. Guet, P. Holza, F. Spiegelman, and F. David (EDP Sciences and Springer-Verlag, Berlin, 2001).

[14] A. V. Korol and A. V. Solov'yov, J. Phys. B **30**, 1105 (1996).

[15] W. Ekardt, Phys. Rev. B **33**, 8803 (1986).

[16] W. Ekardt, Phys. Rev. B **36**, 4483 (1987).

[17] L. G. Gerchikov, A. V. Solov'yov, J. P. Connerade, and W. Greiner, J. Phys. B **30**, 4133 (1997).

[18] L. G. Gerchikov, A. N. Ipatov, and A. V. Solov'yov, J. Phys. B **30**, 5939 (1997).

[19] L. G. Gerchikov, A. N. Ipatov, A. V. Solov'yov, and W. Greiner, J. Phys. B **31**, 3065 (1998).

[20] T. Ditmire, Contemp. Phys. **38**, 315 (1997).

[21] L. G. Gerchikov, A. N. Ipatov, R. G. Polozkov, and A. V. Solov'yov, Phys. Rev. A **62**, 043201 (2000).

[22] J. P. Connerate, L. G. Gerchikov, A. N. Ipatov, and A. V. Solov'yov, J. Phys. B **31**, L27 (1998).

[23] J. P. Connerate, L. G. Gerchikov, A. N. Ipatov, and A. V. Solov'yov, J. Phys. B **32**, 877 (1999).

[24] S. Sentürk, J. P. Connerade, D. D. Burgess, and N. J. Mason, J. Phys. B **33**, 2763 (2000).

[25] L. D. Landau and E. M. Lifshitz, *Quantum Mechanics* (Pergamon, London, 1965).

[26] A. B. Migdal, *Qualitative Methods in Quantum Mechanics* (Nauka, Moscow, 1983).

[27] D. A. Varshalovich, A. N. Moskalev, and V. K. Khersonskii, *Quantum Theory of Angular Momentum* (World Scientific, Singapore, 1988).

[28] A. A. Lushnikov and A. J. Simonov, Z. Phys. **270**, 17 (1974).

[29] T. L. Ferrell and P. M. Echenique, Phys. Rev. Lett. **55**, 1526 (1985).

[30] T. L. Ferrell, R. J. Warmack, V. E. Anderson, and P. M. Echenique, Phys. Rev. B **35**, 7365 (1987).